

Assessment of the Structure and Core Losses Pertaining to Magnetic Toroids Made from Powder and Cast in One Production Step

MARCIN NABIALEK^{1*}, JAN FUZER², LUBOSLAVA DAKOVA², PAWEŁ PIETRUSIEWICZ¹

¹ Institute of Physics, Faculty of Production Engineering and Materials Technology, Czestochowa University of Technology, 19 Armii Krajowej Str., 42-200 Czestochowa, Poland

² Institute of Physics, P.J. Safarik University, Park Angelinum 9, 040 23 Kosice, Slovakia

This paper presents the results of a comparison of two methods for the preparation of permalloy-type material. The nominal blend composition was Ni80-Fe14.7-Mo4.5-Mn0.5-Si0.3. Samples were prepared in the form of toroids using powder metallurgy and an induction casting method. The following measurements were carried out on samples: computer tomography, VSM, XRD, and measurement of the total magnetic losses at different frequencies and the magnetic induction. Both technologies were found to create a crystalline material with similar phases. The sample prepared by the induction casting method exhibited high coercivity, low magnetization saturation and high excess losses in comparison with the sample that had been subjected to a 24h and 120h milling duration.

Keywords: magnetic cores, permalloy, core losses, milling process

Electrotechnical alloys have been undergoing improvements for decades, and these enhancements lead to better properties [1]. One group of interesting materials that is widely used in the electrical industry is the so-called group of 'permalloys' [2]. These materials are characterized by: low core losses, and high initial and maximum permeability values compared with commercially available iron and silicon alloys [3]. Permalloy alloys are quite 'plastic' and can be produced in the form of thin tapes at high cooling rates or using powder metallurgy with a selected shape [4]. For both of these methods, it is important to use pure ingredients - in the right proportions. Iron-silicon materials with an increased silicon content, starting from 4%, become brittle and lose their good mechanical properties; this problem greatly limits their applicability. As mentioned previously, one of the most important determinants of the suitability of an electrotechnical alloy material is the total core losses [5-9].

Total core losses (P_t) on the magnetization cycle in magnetic materials should be divided into three components [10-13]: hysteresis losses (P_{his}), eddy current losses (P_{cl}) and additional losses (P_{exc}):

$$P_t = P_{his} + P_{cl} + P_{exc} \quad (1)$$

In general, the hysteresis loss corresponds to the hysteresis loop, measured at low frequency, and is usually measured directly from the hysteresis loop area. However, in the case of soft magnetic materials belonging to the permalloy group, this is quite a difficult task; this is because the determined field is very small for the greater values of induction and small changes in the value of the rising and falling portions of the hysteresis loop. When calculating the losses from hysteresis per unit volume, it is often assumed that (over one full cycle) these losses are independent of frequency. P_{his} is calculated on the basis of Steinmetz's equation:

$$P_{his} = \eta B_1 \max \uparrow n \quad (2)$$

where: B_{\max} - maximal induction, η and n are constants.

The loop losses arising from magnetic hysteresis are a function of the sample thickness and are associated with irreversible magnetization processes that are influenced by the pinning centres that inhibit motion of the domain walls.

For an homogeneous distribution of the magnetic flux density within the cross-section of the measured material [14, 15]:

$$P_{cl} = \frac{(\pi 2af B_{\max})^2}{6\rho} \quad (3)$$

where:

$2a$ - sample thickness;

f - field frequency;

ρ - resistivity (by volume).

The value of the eddy current loss is proportional to the square of the sample thickness, frequency and induction, and inversely proportional to the resistivity (with the constraint that the product ap is small). In this case, equation (3) is acceptable. Of course, such assumptions are appropriate for materials produced by powder metallurgy for use as magneto-dielectrics; i.e. with constant permeability. This means that the sinusoidal nature of the waveform and induction of eddy currents within the sample are directly related to the operating sinusoidal field. It should also be noted that the linearity of the B and H dependencies is not preserved, which, in a sense, is not entirely consistent with the above statement; but in calculations, this fact has no significant effect on the value of the losses, both from hysteresis and from eddy currents. The contribution of eddy currents in the hysteresis phenomenon is closely related to the domain structure: specifically to the ratio of the magnitude of ferromagnetic domains to the thickness of a given sample. For ferromagnetic domains, very small calculated values based on the theory are consistent with those obtained empirically. It should also be taken into consideration that the distribution of eddy currents within the sample volume is different from that of the theory.

* email: nmarcell@wp.pl

The last term of the equation (1) defining additional losses can be described approximately as follows [13]:

$$P_{exc} = 8.76 \cdot \sqrt{\sigma G S V_0} B_{peak}^{3/2} f^{3/2} \quad (4)$$

where:

G- adimensionless factor;

S - cross-section of the sample;

V_0 - constant associated with the impact of the pinning centres on the domain walls. Additional losses are mainly related to migrational relaxation and, to a lesser extent, to frequency and temperature.

In the case of iron alloys, various additives are added to increase the maximum saturation value. Depending on the content of iron and nickel in the alloy and its temperature, these alloys are characterized by a different unit cell arrangement. Iron alloys have a spatially centred network of regular systems, whereas alloys with a higher nickel content have a face centred network [16]. Increases in the saturation values and improvement of the soft magnetic properties can be achieved by the addition of silicon, molybdenum or manganese to the alloy's composition [17]. In pure nickel, there is about 0.6 non-compensated electron spin per atom, which is 0.6 Bohr magnetons per atom, describing the state of saturation. The reason for this fact is the incomplete filling of the third subshell of the atom; this needs 10 electrons (5 spin-up and 5 spin-down) to fill it. In fact, there are 5 electrons with an up-spin and an average of 4.4 electrons with a down-spin, which defines a gap of 0.6 electrons. This gap is the cause of the magnetic moment of the atom. This means that the partial filling of this gap, for example by foreign dopants, will reduce saturation. The silicon in the third incomplete subshell contains 4 electrons, which should considerably reduce saturation. It has been assumed generally that non-magnetic alloy additives should reduce the saturation of alloys due to the thinning of the magnetic structure. The permalloys with the addition of Mn are quite different; for these, the magnetization of the alloy increases. Alloys having a high nickel content, i.e. approximately 82%, and without undergoing the proper treatment process, exhibit relatively high magnetostriction [18]. The main advantage of permalloys is their high magnetic permeability. Initially, the magnetic permeability of iron-nickel alloys was increased by a heat treatment process of 1 h duration at 900-1000°C, followed by very slow cooling to room temperature. For such melt alloys, it has been noted that, an additional increase in magnetic permeability can be obtained through an additional reheating treatment [19]. In this case, heating of the alloy was carried out already at 600°C and with a significantly increased cooling rate. This point of reference should refer to the high magnetostriction value for these alloys, which tends almost to zero after thermal treatment [20]. This fact results from the relationship, described by Becker, of: initial permeability, saturation magnetization, saturation magnetostriction and Young's modulus. Theoretically, it was shown that magnetostriction falls to zero when permeability tends to infinity.

The paper presents the results of studies into the: structure, magnetic permeability and magnetization losses for permalloy samples. These samples were produced by melting selected alloy components, injecting the melt into a copper mould, and applying powder metallurgy using two grinding times: 24 h and 120 h.

Experimental part

Test samples were fabricated from high-purity components, i.e.: Fe - 99.99% at, Ni, 99.98% at, Si, 99.98%

at, Mo - 99.98% at, and Mn-99.99% at. The rapidly-cooled sample was obtained in two steps. In the first production phase, the alloy components were melted in an arc furnace under a protective gas atmosphere (Ar). The alloy ingots were melted several times from both sides. In addition, titanium was used as an absorbent for the remaining oxygen in the working chamber. Then the ingots were divided into smaller portions, which were melted in an induction furnace. The investigated specimens were produced in the form of rapidly-cooled toroids by injecting the melt into a copper mould. Chemical constituents for the production of cores using powder metallurgy had the same purity as those used to produce rapidly-cooled cores. After weighing-out the appropriate proportions, the powdered ingredients were placed in a planetary mill and subjected to 24 h and 120 h grinding. The powder thus obtained was divided into two equal portions. One was heated at 600°C and mixed with the other. Then the blended powders were cold-pressed in a hydraulic press. Powder pressing was carried-out unidirectionally in one axis. After obtaining the toroids, they were subjected to an annealing process at 1200°C for 60 min. The structure of the samples was tested using a BRUKER D8 ADVANCE X-ray diffractometer equipped with a (CuK α) cathode. Samples were exposed within a 2 θ -angle from 30 to 120° at a resolution of 0.02° and using an exposure time of 5 s. The crystalline phases occurring within the volumes of the samples were determined using the most recent COD base. The internal structure was examined using computer tomography. 3-D visualization of the scanned samples was carried out using Bruker SkyScan software. The X-ray parameters, such as: voltage, type of filter, exposure time and pixel size, were optimized in order to obtain the best image contrast. The X-ray tube voltage was 100 kV and the current was 100 μ A. The X-ray projections were obtained at 0.3° intervals with scanning angular rotation of 360°; six frames were averaged for each rotation. The resolution was pixel size = 2.38 μ m. In addition, ring artefacts were reduced through the selection of a random movement amplitude of 50. Exposure time was 1200 ms. The images were reconstructed and analysed using Bruker NRecon and CTAn software. Bruker DataViewer and Bruker CTVol were used to display the microstructures of samples.

The total core losses of samples were measured over the frequency range of: 50 Hz to 1000 Hz by means of an automated system FERROMETER for toroidal samples.

Static magnetic hysteresis loops were measured using a vibration magnetometer (VSM, Lake Shore 7301) operating in a magnetic field of up to 2 T for powdered samples. All measurements were made at room temperature.

Results and discussions

Figure 1 shows the X-ray diffraction patterns for the toroidal samples.

On each of the diffractograms, clear peaks are visible - corresponding to the crystalline form [21]. Based on an analysis of Roentgen's diffraction patterns, made using the Match program with a base COD (Crystalline Open Database), the crystalline phases present in the volume of the samples were identified: FeNi₃, Fe₂O₄ and Ni_{0.91}Mo_{0.09}. In the X-ray diffraction images obtained from the rapidly-cooled sample, clearly separated peaks of similar positions can be seen. This is probably due to insufficient homogenization of the sample during the melting process. During the solidification of the sample, an additional phase was generated in addition to the expected FeNi₃ phase: Ni_{0.91}Mo_{0.09}. For the powdered metallurgical samples,

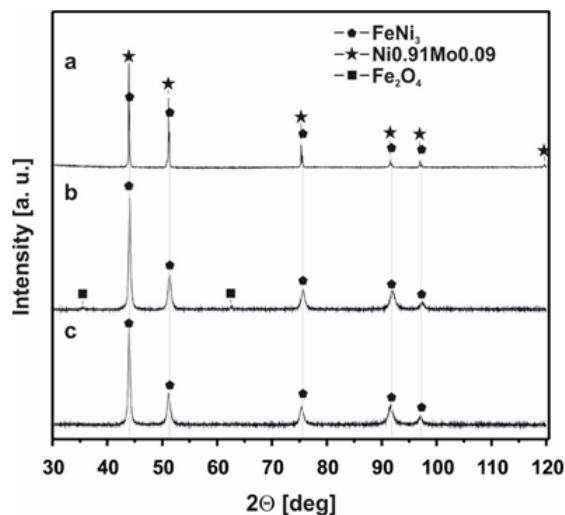


Fig. 1. X-ray patterns obtained for the investigated samples: a - rapidly-cooled toroid, b - core made from powder that had been ground for 24 h, c - core made from powder that had been ground for 120 h

no Ni_{0.91}Mo_{0.09} phase was found. However, for a sample ground over a period of 24 h, in addition to the FeNi₃ phase, Fe₂O₄ also appeared; however, with increased grinding time (to 120 h) this latter phase decomposed. Based on chemical composition analysis using EDS secondary electron diffraction, it was found that within the volume of all samples there were no areas in which there were any unmixed components. This indicates that multi-hour milling leads to effective mixing of alloy components. Despite the cleanliness of the milling process in the volume of the melt, a trace amount of oxides was produced.

Properties of the investigated alloy vary depending on its construction. In order to reveal the internal structure of samples made by powder metallurgy, computer tomography was performed. Figure 2 presents three-dimensional reconstructions of samples made using powder metallurgy.

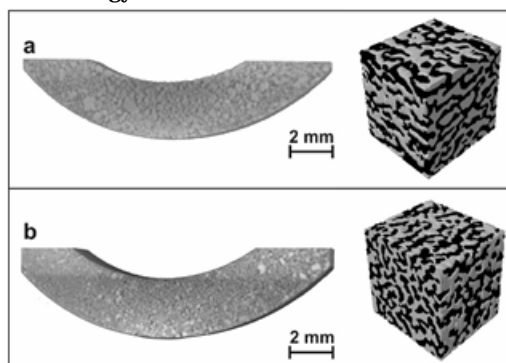


Fig. 2. Three-dimensional image reconstructions for powdered samples: a-toroidal powdered 24 h, b- toroidal powdered 120 h

Based on the analysis of the three-dimensional reconstructions of the images, it can be stated that the tested samples have a high porosity - of up to several dozen percent. Despite such a high proportion of excess volume, the samples are consistent. In the present state, it is difficult to determine the size of components made by powder metallurgy. It can only be concluded that the particles forming the toroid range from several dozen to more than 100 microns. The important parameters determining the usefulness of electrotechnical alloys are: the saturation magnetization and the coercive field. Figure 3 shows static magnetic hysteresis loops.

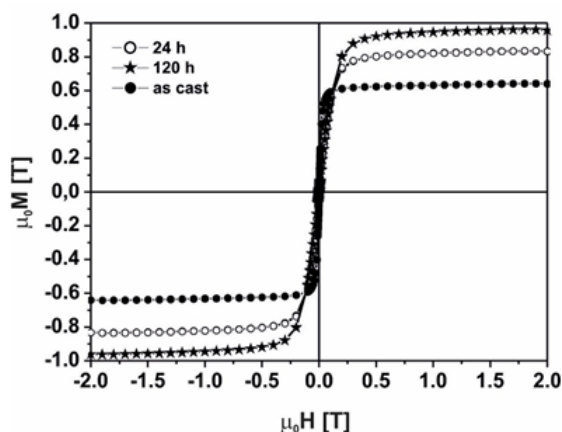


Fig. 3. Static magnetic hysteresis loops for the samples produced by rapid-cooling and powder metallurgy

Based on the static magnetic hysteresis loop analysis, the saturation magnetization and coercive field were determined (table 1).

Table 1
THE H_c AND μ₀M VALUES OBTAINED FROM STATIC ANALYSIS OF THE MAGNETIC HYSTERESIS LOOPS FEATURED IN FIGURE 3

Sample	H _c [a/m]	μ ₀ M [T]
As-cast	380	0.639
24 h	40	0.831
120 h	48	0.956

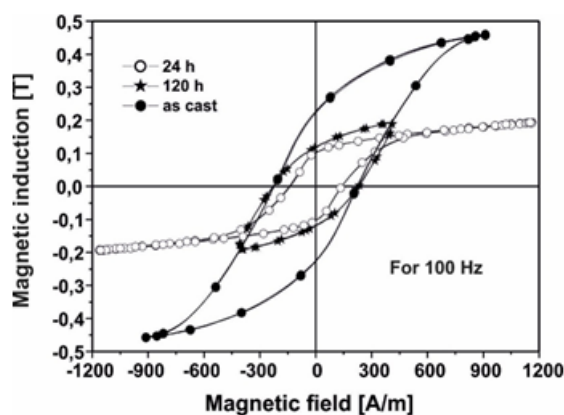


Fig. 4. Quasi-static magnetic hysteresis loops for the test alloy, recorded for a magnetizing field frequency of 100 Hz

The shape of the measured static magnetic hysteresis loops is typical for ferromagnetic alloys with soft magnetic properties [22-24]. The highest value of saturation magnetization was found in the sample that had been subjected to 120 h of milling; in volume of these samples, only the crystalline phase FeNi₃ was observed. The coercion field values were found to be similar for samples milled over 24 h and 120 h periods. By far the worst soft-magnetic properties were exhibited by samples produced by the casting method - which was not stress-relieved. The milled samples were powdered *composites*, composed of powders in the milled state and that following heating in 1:1 proportions. In addition, after the powders were mixed, the resulting toroid was reheated. The 'soaking' process itself played a major role in the formation of the magnetic properties and was intended to relax the structure [25].

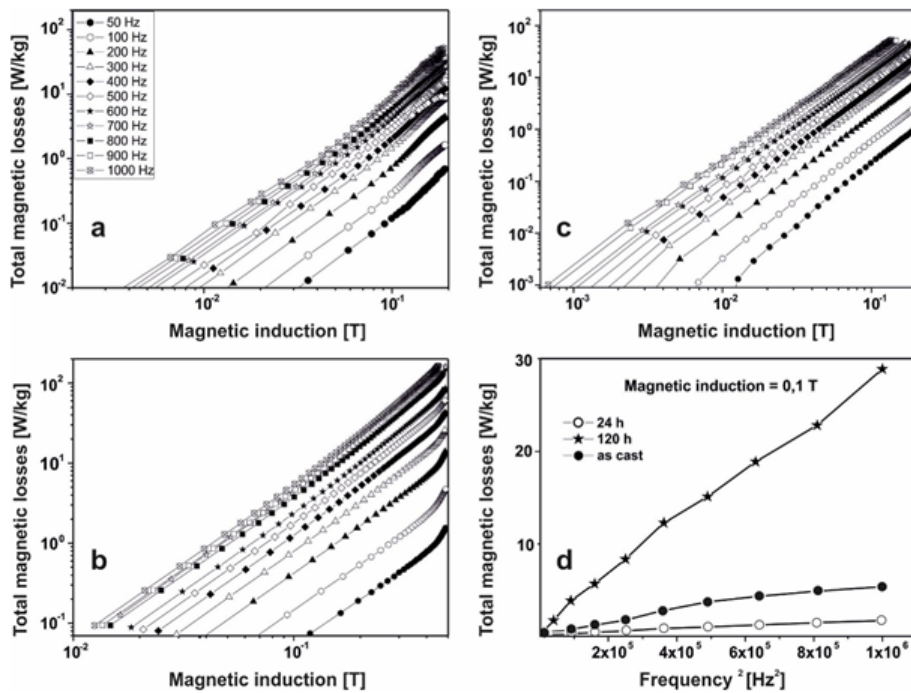


Fig. 5. Total core losses (as a function of maximum induction and loss of magnetization as a function of the frequency squared, with constant magnetic induction) for samples of the alloy produced by rapid-cooling and powder metallurgy: a - rapidly-cooled toroid, b - core ground for 24 h, c - core ground for 120 h

Another very important electrical parameter is the total core loss, which is determined by measurements made for different frequencies of the magnetizing field. Figure 4 shows exemplary quasi-static magnetic hysteresis loops for the investigated alloy at the selected frequency of the magnetizing field.

Figure 5 shows the relationship of the core losses as a function of the maximum induction - for the three test samples of the investigated alloy.

For all of the investigated samples, the graph-plot of total core loss as a function of maximum induction is typical for electrotechnical materials. An increase in total losses for demagnetization is observed with increasing frequency of the magnetizing field [25, 26].

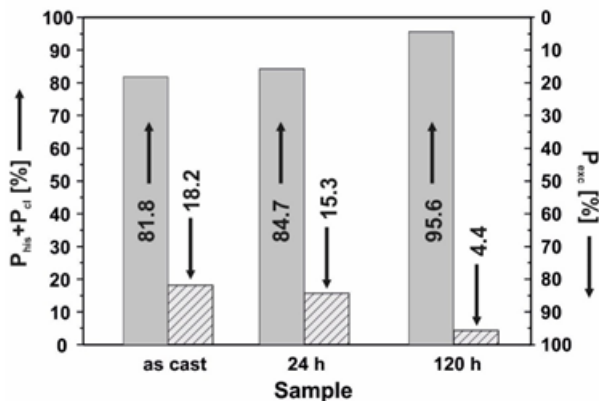


Fig. 6. Contribution of: hysteresis, eddy currents and additional losses to total core losses for samples of the alloy produced by the rapid cooling and powder metallurgy.

For all samples, with a square of the magnetizing field frequency, there was an increase in core losses. It can be seen that the relationship of P / f^2 for fixed magnetic induction is not linear, which means that additional losses occurring in individual demagnetisation cycles [27] should be considered. Figure 6 shows the distribution of losses from hysteresis, eddy currents and additional losses.

The share of additional losses for the samples ranged from a few percent to nearly 20%. The lowest calculated losses were obtained for the powdered sample that had been ground for 120 h - 4.4%, and the highest for the powdered core that had been ground for 24 h - 18.2%. In

the case of the rapidly-cooled toroid material, the additional losses were slightly lower than for the powdered core that had been ground for 24 h and their contribution to the total losses was 15.7%.

Conclusions

In permalloy alloys, a high magnetic permeability and narrow hysteresis loop is expected, with concomitant low total core losses. In such alloys, the weak point is their low magnetization, which can be increased by the introduction of various alloy additives in an amount not exceeding several% at., together with an appropriately performed thermal treatment. In the alloys investigated in this paper, Mo, Mn and Si additives were used to increase the saturation magnetization. The distribution of these additives within the melt depends on the sample itself. The first group of samples was formed by the long-term grinding of the powdered components and their subsequent compression after a previous thermal treatment. The second group of samples was obtained by a rapid-cooling process. The structures of the aforementioned alloys are similar, and the dominant crystalline phase within their volume is the phase FeNi_3 . However, the different manufacturing parameters for each of the alloy samples tested were the reason for the additional configuration of the Fe and O atoms and Mo and Ni atoms. For the 24 h grinding process, a crystalline Fe_3O_4 phase was identified in the volume of the sample - which could be expected. Extending the milling time to 120 h was the reason for the breakdown of the Fe systems with O. For the increased energy pertaining to extended grinding times, the formation of Fe-Ni systems was favoured - which was observed. In the rapidly-cooled alloy, well-defined peaks of similar 2θ position correspond to the phases: FeNi_3 and $\text{Mo}_{0.09}\text{Ni}_{0.91}$. As a result, there was probably insufficient mixing of the alloy components in the first phase of the sample production cycle, or the cooling rate of the melt itself was so large that the solidification time was insufficient for the redistribution of Mo throughout the volume of alloy - which was the reason for the formation of Mo and Ni. The negative mixing heat for pairs of Mo and Ni (-7) atoms is significantly lower than that for pairs of Ni and Fe (-2) atoms - which is the reason for the rapid combination of the Mo with Ni. This is the

reason for the uneven distribution of the ingredients in the alloy. In the case that all Mo is used to produce the Ni_{0.91}Mo_{0.09} crystalline phase, the Ni content remains within the volume of alloy; for this situation, according to the Fe-Ni phase diagram, it is most advantageous to form the systems $\alpha(\text{Fe, Ni}) + \text{FeNi}_3$. The analysis of microstructure gives many answers about the properties of electrotechnical alloys, so it should always be considered and compared to the properties of the produced materials. Therefore, the most interesting aspect of this work is the comparison of the magnetic toroid properties obtained by two methods. It is important to note here the filling within the sample volume. Much better filling was observed for an injection moulded toroid, for which no defects in the form of pores were observed. It is hard to believe that the porosity of powder cores is at the level of several dozen percent, as indicated by the results of the computer tomography. Reduced filling is not a desirable effect and can affect the results of the magnetic measurements and the service life of the material. Permalloy alloys exhibit low magnetostriction. Lack of this feature gives the possibility of fail-safe use of powdered low magnetic toroids for operation at various frequencies. The actual value of the saturation magnetization and coercive field was measured for the powders obtained with VSM and it was found that, despite the same chemical composition, differences in the values of these parameters were observed. These differences are related, inter alia, to the varying degree of relaxation of their magnetic structure and the presence of the crystalline phases present in the samples tested. As shown in table 1, the saturation magnetization of the samples produced from the powders was greater than that of the molten cast sample and the coercive field value was nearly ten times smaller. The paper presents primarily the results of the study of total core losses with separation for losses from hysteresis and eddy currents and additional losses. Interestingly, the resulting liquid-phase sample exhibited core losses comparable with a powdered-ground-for-24 h sample, and significantly smaller than for the powder sample that had undergone 120 h of milling. This fact raises the question of which mechanisms are critical in the formation of the magnetic structure of the investigated permalloy sample. The powder samples were manufactured under identical conditions. The only distinguishing factor was the grinding time. It can be assumed that, as a result of the extended grinding process - which is a high-energy process - there has been better homogenisation of the melt components in the coated particles featuring dimensions substantially smaller than those obtained from the powder that had been ground over the shorter duration. The free flow of magnetic flux through the sample is conditioned by the form of the magnetic structure. If domain walls are inhibited by defects in structure or non-homogeneity occurring in the volume of the sample, the total core loss will increase.

References

1. SHOKROLLAHI H., JANGHORBAN K., *J. Mater. Process. Technol.*, 189, nr.1-3, 2007, p. 1

2. BAS J. A., CALERO J. A., DOUGAN M. J., *J. Magn. Magn. Mater.*, 254-255, nr. 255, 2003, p.391
3. MIKLER C.V., CHAUDHARY V., BORKAR T., SONI V., CHOUDHURI D., RAMANUJAN R.V., BANERJEE R., *Mater. Let.*, 190, 2017, p. 9
4. VAJPAI S.K., MAHESH B.V., DUBE R.K., *J. Alloys Compd.*, 476, nr. 1-2, 2009, p. 311
5. YAN Y., MOSS J., NGO K. D. T., MEI Y., LU, G. Q., *IEEE Energy Conversion Congress and Exposition (ECCE)*, 2016, p. 1
doi: 10.1109/ECCE.2016.7854826
6. TANASE S.I., TANASE D., DOBROMIR M., SANDU A.V., GEORGESCU V., *Journal Of Superconductivity And Novel Magnetism*, 29, 2016, p. 469.
7. PASCARIU P., TANASE S.I., TANASE D.P., SANDU A.V., GEORGESCU V., *MATERIALS CHEMISTRY AND PHYSICS*, 131, 2012, p. 81
8. TUGUI C.A., VIZUREANU P., IFTIMIE N., STEIGMANN R., *IOP Conference Series-Materials Science and Engineering*, 147, 2016, UNSP 012040
9. PERJU M.C., TUGUI C.A., NEJENERU C., AXINTE M., VIZUREANU P., *IOP Conference Series-Materials Science and Engineering*, 133, 2016, UNSP 012025
10. PICCIN R., TIBERTO P., CHIRIAC H., BARICCO M., *J. Magn. Magn. Mater.*, 320, nr. 20, 2008, p.806
11. K. BLOCH, *J. Magn. Magn. Mater.*, 390, 2015, p. 118
12. BARBISIO E., FIORILLO F., RAGUSA C., *IEEE Trans. Magn.*, 40, nr. 41, 2004, p.1810
13. PFIUTZNER H., SCHONHUBER P., ERBIL B., HARASKO G., KLINGER T., *IEEE Trans. Mag.*, 27, nr. 3, 1991, p. 3426
14. JILES D.C., *Introduction to Magnetism and Magnetic Materials*, Chapman and Hall Publishers, first ed., London and New York, 1991 chap. 12,
15. SHEN T.D., XIN S.W., SUN B.R., *J. Alloy. Compd.*, 658, 2016, p. 703
16. KURU H., KOCKAR H., ALPER M., *J. Mater. Sci.-Mater. El.*, 26, nr.7, 2015, p. 5009
17. KINO E., CHUJO N., KUME K., AOYAMA T., FUKUDA M., *J. Jpn. Soc. Powder. Metall.*, 63, nr. 7, 2016, p. 618
18. HECK C, *Magnetic Materials and Their Applications*, Butterworth & Co. (Publishers) Ltd. Published by Elsevier Ltd, 1974, p. 396
19. GHEISARI K., OH J.T., JAVADPOUR S., *J. Alloys Compd.*, 509, nr. 3, 2011, p. 1020
20. AKOMOLAFE T., JOHNSON G. W., *J. Mater. Sci.*, 23, nr. 3, 1988, p. 790
21. OLEKSAKOVA D., KOLLAR P., FÜZER J., KUSY, M., ROTH S., POLANSKI K., *J. Magn. Magn. Mater.*, 316, nr. 2 SPEC. ISS, 2007, p. e838-
22. BLOCH K., *Arch. Metall. Mater.*, 61, nr. 1, 2016, p. 445
23. NABIAŁEK M., PIETRUSIEWICZ P., BŁOCH K., *J. Alloys Compd.*, 628, 2015, p. 424
24. NABIAŁEK M., BLOCH K., SZLAZAK K., SZOTA M., *Mater. Technol.*, 50, nr. 2, 2016, p. 189
25. FUZER J., KOLLAR P., OLEKSAKOVA, D., ROTH S., *J. Alloys Compd.*, 483, nr. 1-2, 2009, p. 557
26. OLEKSAKOVA D., FUZER J., KOLLAR P., ROTH S., *J. Alloys Compd.*, 333, 2013, p. 18
27. K. BLOCH, *J. Magn. Magn. Mater.*, 390, 2015, p. 118

Manuscript received: 4.01.2017